Assessing the EPIC spectral calibration in the hard band with a 3C 273 observation

Silvano Molendi
IASF/CNR, Via Bassini 15, I-20133 Milano, Italy

Steve Sembay
X-Ray Astronomy Group, Leicester University, LE1 7RH, UK

March 17, 2003

Abstract

We describe the analysis of a simultaneous XMM-Newton BeppoSAX observation of 3C273 carried out in June 2001. Our primary aim is to asses spectral parameters for the high energy (above 3keV) spectrum of EPIC MOS, EPIC PN and MECS and to compare them. We find that in the 3-10 keV band EPIC MOS and PN spectral slopes are contained within a $\Delta\Gamma = 0.03$, with the exception of the MOS1 measurement, which is found to be significantly flatter. The EPIC slopes are in good agreement with those obtained with the MECS on-board BeppoSAX. These results represent a major improvement in our understanding of the EPIC high energy response.

1 MOS Analysis

Event files were processed at LUX by S. Sembay using the publically available SAS 5.4.1 S/W. Our first concern is to determine if pileup is present and to what extent. There are various ways to go about this. One possibility is to use epatplot. We have run epatplot on various annuli centered on the emission peak. In Fig. 1, 2 and 3 we present results for 3 annuli with bounding radii $0''$-$6''$, $6''$-$37.5''$ and $15.0''$-$37.5''$. Clearly annuli including data from the innermost regions are affected by pile-up to some extent. The current version of epatplot is extremely useful to detect pile-up at a glance, however it does not write to file the expected fractions and therefore does not allow to perform a more quantitative analysis.

Moreover, as we shall verify further on, the large discrepancy observed above 2 keV between predicted and measured pattern 0 fractions does not imply that major spectral distortions of the pattern 0 spectrum are occurring at energies greater than ~ 2 keV. At moderate pile up rates such as those occurring in this observation the main effect of pile-up is to take pattern 0 events and turn them into doubles. Piled up pattern 0 events are less likely simply because the probability of producing a piled-up double is 4 times larger than that of producing a piled up single. The major effect on pattern 0 events is a loss of events to higher order patterns (mainly doubles). Since the probability of an event to be lost to pile-up is independent of its energy, the loss of events will result in a lower normalization of the pattern 0 spectrum and not in a distortion of its shape. In epatplot the predicted fractions are computed under the assumption that none of the recorded events are due to pile-up, if however, a certain number of double, triple and quadrupole events are due to pile-up, then the assumed fraction of pattern 0 events will be miscalculated simply because based on an incorrect number of total events. A defect of pat. 0 events is observed above 2 keV because it is at these energies that the effective area starts to drop rapidly and piled-up doubles become a sizeable fraction of all doubles.

1.1 Pattern ratios

Another possibility to assess pile-up is to derive the ratio of doubles to singles spectra for different annuli, we shall indicate with $R_{bivp0}(r_{min}, r_{max})$, the ratio of the spectra for vertical bipixels to pattern 0 from the annulus with bounding radii r_{min},r_{max} and with $R_{bihp0}(r_{min}, r_{max})$ the ratio of the spectra for horizontal bipixels to pattern 0 from the annulus with bounding radii r_{min},r_{max} expressed in arcseconds. For regions unaffected by pile-up the ratio should be the same, while for regions where pile-up is important the ratio should be larger, particularly for those energies where "true" bipixels are expected to be few. To quantify somewhat the above differences, we have computed $R_{bivp0}(0, 3)/R_{bivp0}(6, 37.5)$ and $R_{bihp0}(0, 3)/R_{bihp0}(6, 37.5)$, i.e. a ratio of ratios, this is less complicated than it may appear to be.

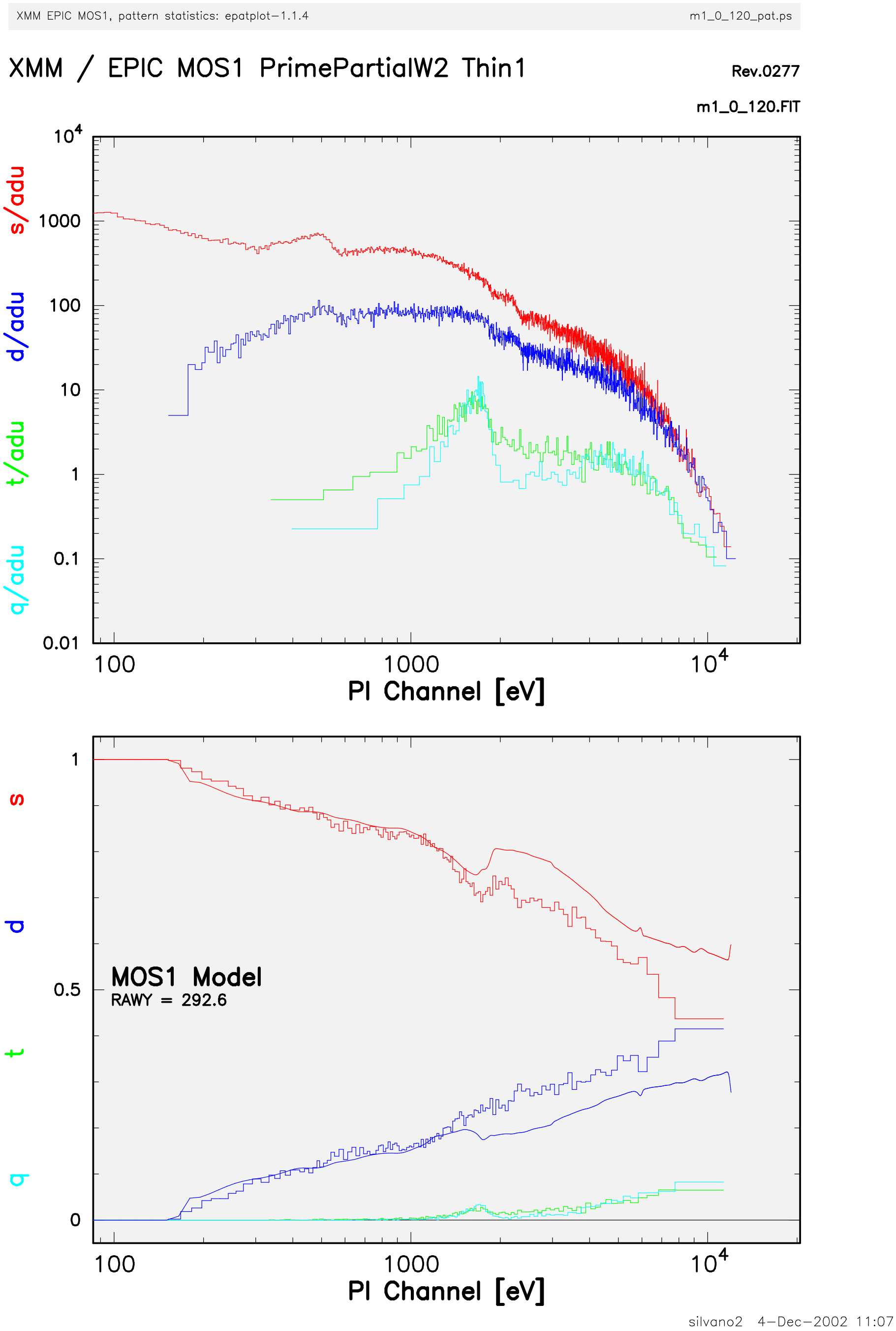

Figure 1: epatplot for a circle with radius 6″

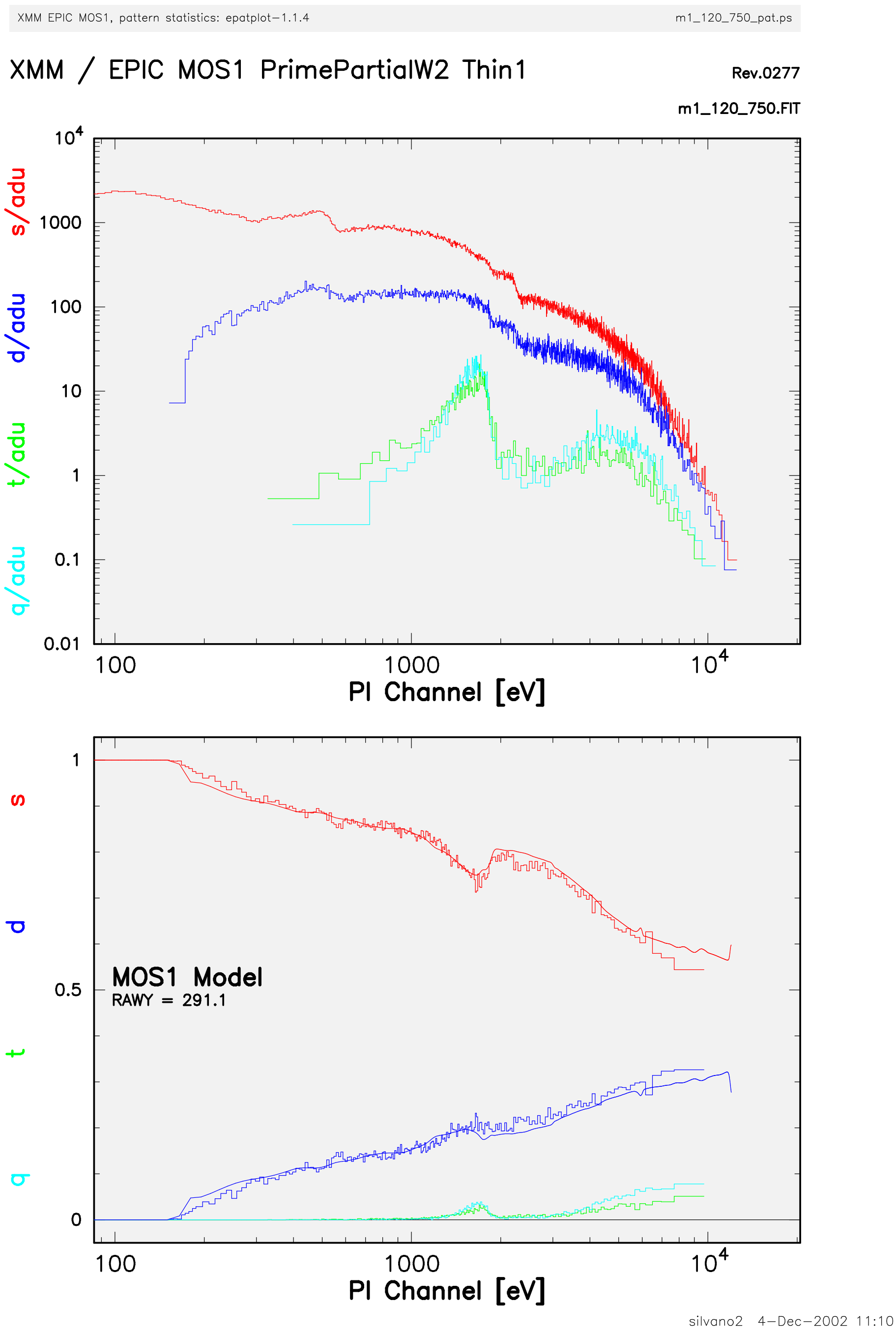

Figure 2: epatplot for an annulus with bounding radii 6″ and 37.5″

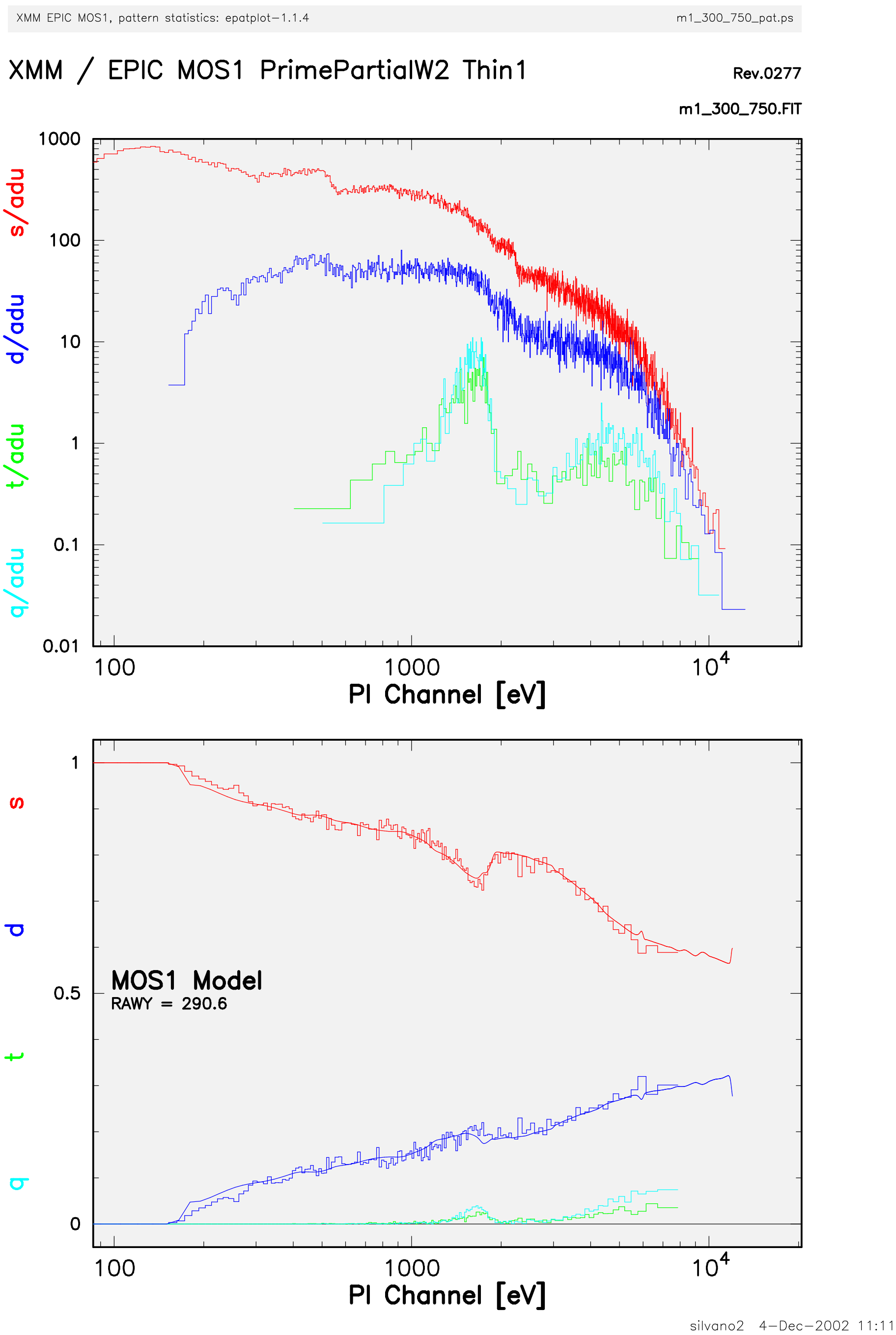

Figure 3: epatplot for an annulus with bounding radii 15″ and 37.5″

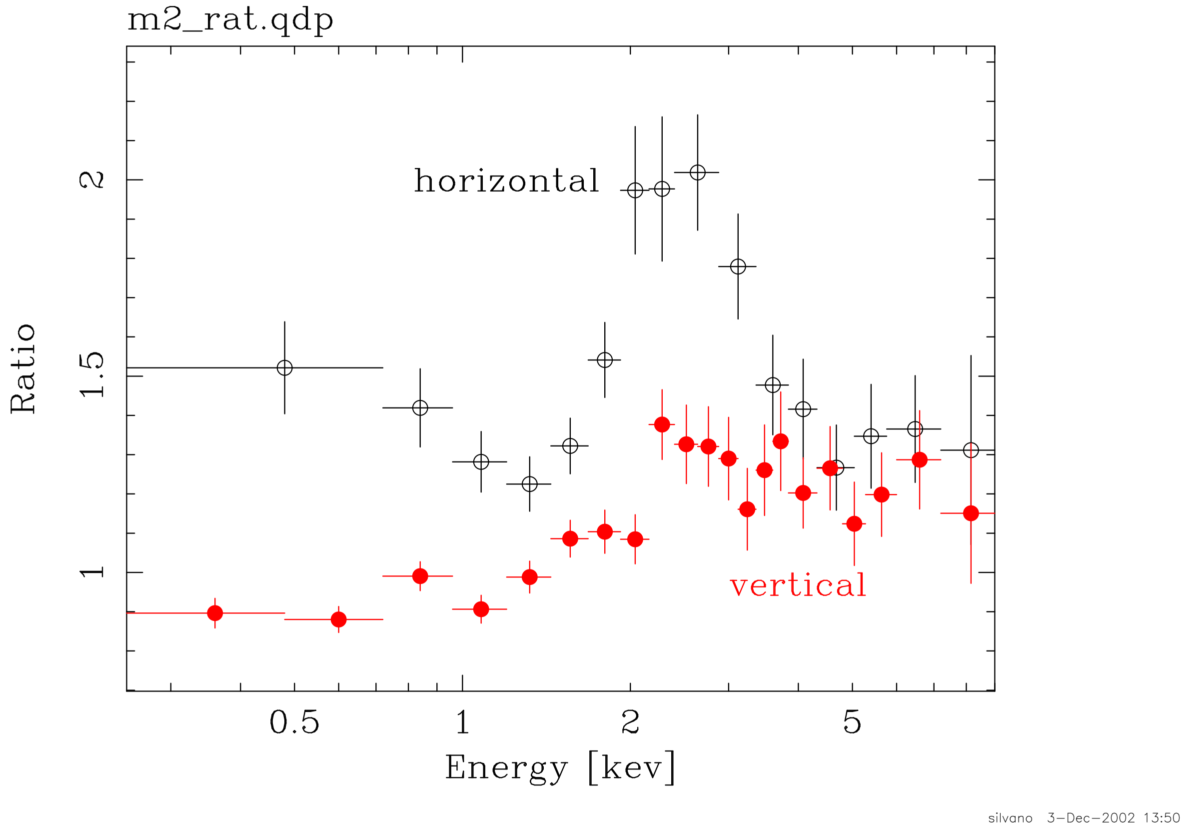

Figure 4: the $R_{bivp0}(0,3)/R_{bivp0}(6,37.5)$ and $R_{bihp0}(0,3)/R_{bihp0}(6,37.5)$ ratio of ratios, see text for details.

In figure 4 we report the above ratio for MOS2, results for MOS1 are very similar. In general the ratios lie above 1 indicating that some pileup is present in the inner circle. Let us go in more detail and consider first vertical bipixels, below about 0.8 keV the ratio is close but slightly smaller than 1 indicating that pile-up is not very important and that the dominant effect is that of a loss of events (most likely to higher order patterns). Around 2.2 keV we observe a jump, this is related to the gold edge. At energies larger than 2.2 keV the effective area is reduced drastically and so is the probability of producing a true bipixel, on the contrary the probability of producing a bipixel through pile is unaffected by the edge, consequently we observe a jump in the ratio due to the increased fraction of piled up bipixels over true bipixels. From about 2.2 keV to 9 keV the ratio remains essentially constant. Let us now consider horizontal bipixels, as we know, the probability of producing a true horizontal bipixel is smaller than that of producing a true vertical bipixels. On the contrary the probability of producing a horizontal bipixel from 2 piled up singles is identical to that of producing a vertical bipixel from 2 piled up singles, thus the fraction of pile up events we observe is larger for horizontal bipixels than it is for vertical bipixels. Most interestingly the ratio evidences a line-like structure emerging between 1.8 and 3 keV. This is due to the combined effect of the Si edge at 1.8 keV and of the Au edge at 2.2 keV. Both these edges reduce drastically the amount of true bipixels while leaving unaffected the amount of piled-up bipixels, thus the ratio goes up. Around 3 keV the ratio starts to drop because piled-up bipixels are now being made in part from monopixels with energies larger than 1.8 keV. Up to this point, the reader may have found the above results amusing but not particularly important. The important part is that a mild pile up, such as the one observed in the core of 3C 273 results in a substantial amount of spurious bipixels in the energy range between 1.8-3 keV. Thus, when fitting pattern 0-12 spectra this will show up as an excess in the 1.8-3 keV energy range. Since the energy range under exam is one where we observe the Si and Au edges the naive calibrator may be lead to thinking that the problem is related to a miss-calibration of the edge depth when it is infact a pile-up problem.

1.2 Pattern 0 vs. patterns 0-12 spectral fitting

Another way of assessing pile up is to fit pattern 0 and pattern 0-12 spectra from different annuli. For spectra including inner regions affected by pile-up fits will yield different results for pattern 0 and pattern 0-12, for outer regions where pile-up is absent they will yield consistent results. In Table 1 we report the result of spectral fits to MOS1 and MOS2 data in 2 annuli with bounding radii $0''$-$6''$, $6''$-$37.5''$. Results are reported in the form of $\Delta\Gamma$ where $\Delta\Gamma \equiv \Gamma_{p0\_12} - \Gamma_{p0}$

Table 1: $\Delta\Gamma \equiv \Gamma_{p0\_12} - \Gamma_{p0}$

Spectrum	$\Delta\Gamma$ 3-10 keV	$\Delta\Gamma$ 4-10 keV
MOS1 $0''$-$6''$	-0.08 ± 0.04	-0.17 ± 0.06
MOS2 $0''$-$6''$	-0.06 ± 0.04	-0.10 ± 0.06
MOS1 $6''$-$37.5''$	0.02 ± 0.03	0.00 ± 0.05
MOS2 $6''$-$37.5''$	0.01 ± 0.03	0.02 ± 0.04

In the inner ring the pattern 0-12 spectrum is flatter than the p0 spectrum. This is due to piled up 0 patterns that are detected mostly as higher order patterns with a spectrum that is harder than the real source spectrum (the energy of the piled up event is the sum of the energies of the 2 or more events that contribute). The pattern 0 spectrum is also affected by piled up event which will harden the spectrum, however in this case the effect is significantly smaller as the probability of producing a piled up valid double is 4 times larger than that of producing a piled up pattern 0. In the outer region the effect of pile up is negligible and the pattern 0 and pattern 0-12 spectra show consistent spectral slopes. It is interesting to note that the epatplot for this outer region (see Fig. 2), show some evidence for pile up, however this is insufficient to introduce measurable spectral distortions in our fits.

Assuming that pattern 0 spectra are not substantially distorted even within the core, we may compare the spectral fits for the two annuli. Since each spectrum is analyzed using an effective area appropriate for the specific choice of bounding radii, an agreement between spectral parameters would indicate that the PSF correction is working properly. In Table 2 we report $\Delta\Gamma$ where this time $\Delta\Gamma \equiv \Gamma_{p0}(0'' - 6'') - \Gamma_{p0}(6'' - 37.5'')$

Table 2: $\Delta\Gamma \equiv \Gamma_{p0}(0'' - 6'') - \Gamma_{p0}(6'' - 37.5'')$

Detector	$\Delta\Gamma$ 3-10 keV	$\Delta\Gamma$ 4-10 keV
MOS1	0.21 ± 0.04	0.10 ± 0.06
MOS2	0.21 ± 0.04	0.10 ± 0.05

Results for MOS1 and MOS2 are similar, for both detectors we find that the spectrum extracted from the core is significantly steeper than the one extracted from the wings. The obvious conclusion is that the PSF correction does not work properly. The reader is cautioned that this does not imply that the PSF correction does not work in general. The current PSF calibration is the result of a detailed analysis of the radial profiles of many different sources observed with EPIC (Ghizzardi 2002) and for the typical case of a non-piled up source with an extraction radius of $20'' - 40''$ and no hole in the center it does work adequately.

1.3 Diagonal Patterns

Yet another way of assessing the role of pile up is to consider diagonal bipixels (patterns 26-29). The main advantage of diagonal bipixels is that they are produced virtually only from the pile up of 2 single events. Consequently diagonals can be used to estimate the importance of pile-up. In Fig. 5 we compare the image of 3C 273 in diagonal patterns with the one derived for 0-12 patterns. The source is clearly visible in diagonals and the surface brightness more peaked than in the standard patterns indicating, once again, that some pile-up is present.

The effect of pile up can be split into two different parts. There is a gain of events, and a loss of events, generally speaking the events which are gained have energies larger than those that are lost as the former are made from the sum of the latter.

Let us now for simplicity's sake concentrate on pattern 0 events and assume that the only form of pile-ups are two photon pile-ups (i.e. we neglect pile-ups due to 3 or more events). Following the above arguments the spectrum of observed singles $S_{obs}(E)$ per frame per pixel may be written as:

$$S_{obs}(E) = S(E) - S_{lost}(E) + S_{gain}(E), \quad (1)$$

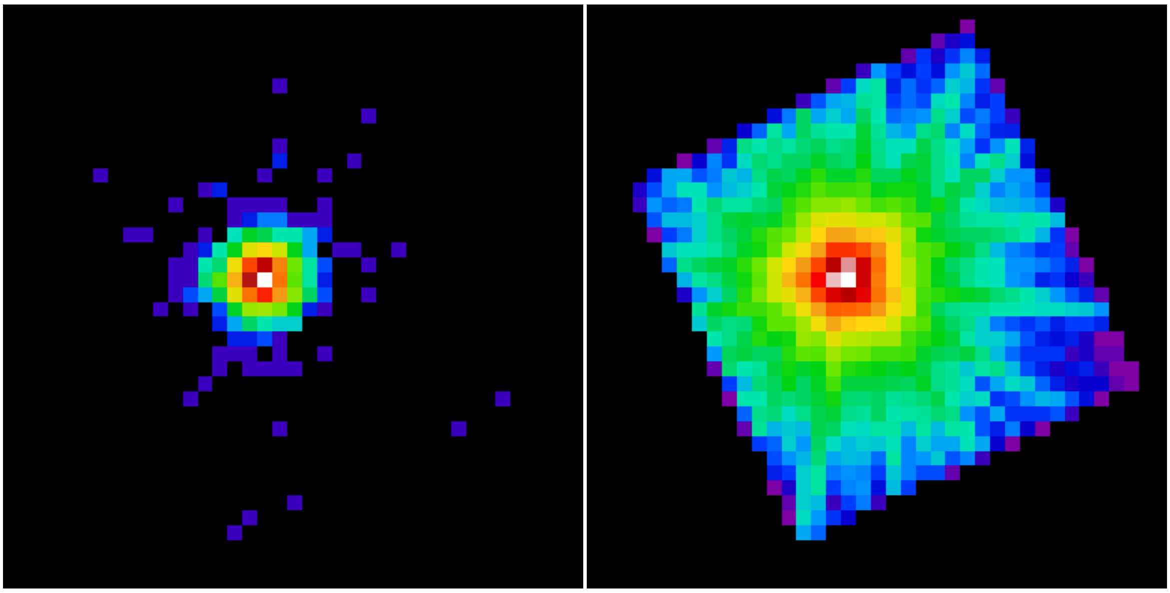

Figure 5: image of 3C 273. **Left panel** image in diagonal patterns; **right panel** image in 0-12 patterns

where $S(E)$ is the pattern 0 spectrum in the no pile-up limit, $S_{lost}(E)$ is the spectrum "lost" to singles and higher order pattern pile-ups and $S_{gain}(E)$ is the spectrum gained from single-single pile-ups. Both the spectrum of events gained $S_{gain}(E)$ and lost $S_{lost}(E)$ from pile-up can be estimated from the spectrum of diagonal events (patterns 26-29). To avoid confusion we shall call $S_{dia}(E)$ the spectrum observed in diagonal patterns and $S_{dia\_p0}(E)$ the spectrum of pattern 0 reconstructed by splitting each diagonal event into two pattern 0 events. It can be shown that

$$S_{gain}(E) = \frac{1}{4} S_{dia}(E), \tag{2}$$

similarly $S_{lost}(E)$ may be related to $S_{dia\_p0}(E)$ through the equation:

$$S_{lost}(E) = \frac{\gamma_1}{4\alpha_1} S_{dia\_p0}(E), \tag{3}$$

where $\gamma_1 = 9 + 3\alpha_2 + 6\alpha_3 + 7\alpha_4$ and α_1, α_2, α_3 and α_4 are the fraction of events giving rise to monopixels, bipixels tripixels and quadripixels in the no pile-up limit. A derivation of Eq. (2) and (3) will be given in Appendix A. As shown in Appendix B Eq. (2) and (3), which are derived in the case of a source illuminating the MOS CCDs homogeneously, can be extended to a generic point source with a surface brightness described by the MOS PSF. Thus we may write:

$$\bar{S}(E) = \bar{S}_{obs}(E) + \frac{\gamma_1}{4\alpha_1}\bar{S}_{dia\_p0}(E) - \frac{1}{4}\bar{S}_{dia}(E), \tag{4}$$

where $\bar{S}$ indicates the spectrum per frame per pixel averaged over the source surface brightness distribution of the source. Since α_1, α_2, α_3 and α_4 depend upon energy, mean values where derived by averaging over the whole MOS spectral range using a 3C 273 spectrum accumulated in the wings of the PSF where no pile-up is present. Derived values are $\alpha_1 = 0.8208$, $\alpha_2 = 0.1623$, $\alpha_3 = 0.0069$ and $\alpha_4 = 0.0100$.

Before applying Eq. (4) to our data we need to consider one last technical issue, when running emchain with the default parameters diagonal patterns are recognized and split into pattern 0 events, they are however flagged and consequently $\bar{S}_{dia\_p0}(E)$ can be easily extracted from the MOS event files. On the contrary to derive $\bar{S}_{dia}(E)$ diagonal patterns must not be split. An easy way to do this is to run the emchain in the following fashion: `emchain emevents:splitdiagonals=N`.

In Table 3 we report the results of spectral fits to MOS1 and MOS2 spectra extracted from a circle with a radius of 37.5″. For each detector we report results for 3 spectra, the first is accumulated from patterns 0-12, the second and third are accumulated from pattern 0 only. Of the pattern 0 spectra the first is not corrected for pile-up effects, while the second is corrected using the pattern 26-29 spectrum as indicated in Eq. (4).

Clearly there is a difference between pattern 0-12 spectra and pattern 0 spectra, this is due to piled-up events present in the patterns 1-12 which harden the pattern 0-12 spectrum. The difference between the uncorrected and the corrected pattern 0 spectra is small indicating that at the moderate counting rate of 3C 273 pattern 0 spectra are only mildly distorted from pile-up.

Table 3: comparison of spectral fits to MOS1 and MOS2 data

Detector	Γ 3-10 keV	Γ 4-10 keV
MOS1 pat0-12	1.50 ± 0.02	1.50 ± 0.03
MOS1 pat0	1.54 ± 0.02	1.62 ± 0.03
MOS1 pat0 diacor	1.57 ± 0.02	1.67 ± 0.04
MOS2 pat0-12	1.57 ± 0.02	1.52 ± 0.03
MOS2 pat0	1.62 ± 0.02	1.63 ± 0.03
MOS2 pat0 diacor	1.65 ± 0.03	1.70 ± 0.04

2 PN

PN event files were generated by M. Freyberg using the version of epchain available at MPE in November 2002. Spectra and response matrices were produced by F. Haberl, the response matrices are coded as **PN6.3_dec02**. we have verified a posteriori that running SAS 5.4.1 on the ODF files we derive consistent results.

The nominal frame-time for the PN small window is 5.67 ms. Taking into account that the PN pixels are about 16 times larger than the MOS pixels, that the MOS frame-time in SW is 0.3 s and that the MOS2 and PN count rates are respectively 17.5 and 70 cts/s, we find that the PN counts per frame per pixel are about the same of those of either MOS1 or MOS2. Since the MOS pile-up on singles is small we expect that this will also be the case for PN singles; a modest pile-up may affect PN doubles which are of course more sensitive than singles. This conclusion is confirmed by the epatplot analysis. In Fig. 6 we report the epatplot for a circle with a $40''$ radius centered on the emission peak. The small discrepancy seen below 600eV is related to a PN calibration issue currently under investigation and not related to pileup. A real pile up problem would show up as a double excess (and single defect) above 1-2 keV, no such effect is seen. Some discrepancy is observed above 8 keV, however similar discrepancies have been observed before and are probably not related to pile up.

We have performed power-law fits in the 3-10 keV and 4-10 keV band for singles and doubles for 3 different extraction regions: a circle with a $40''$ radius and two annuli with bounding radii $5''$-$40''$ and $10''$-$40''$. Results are

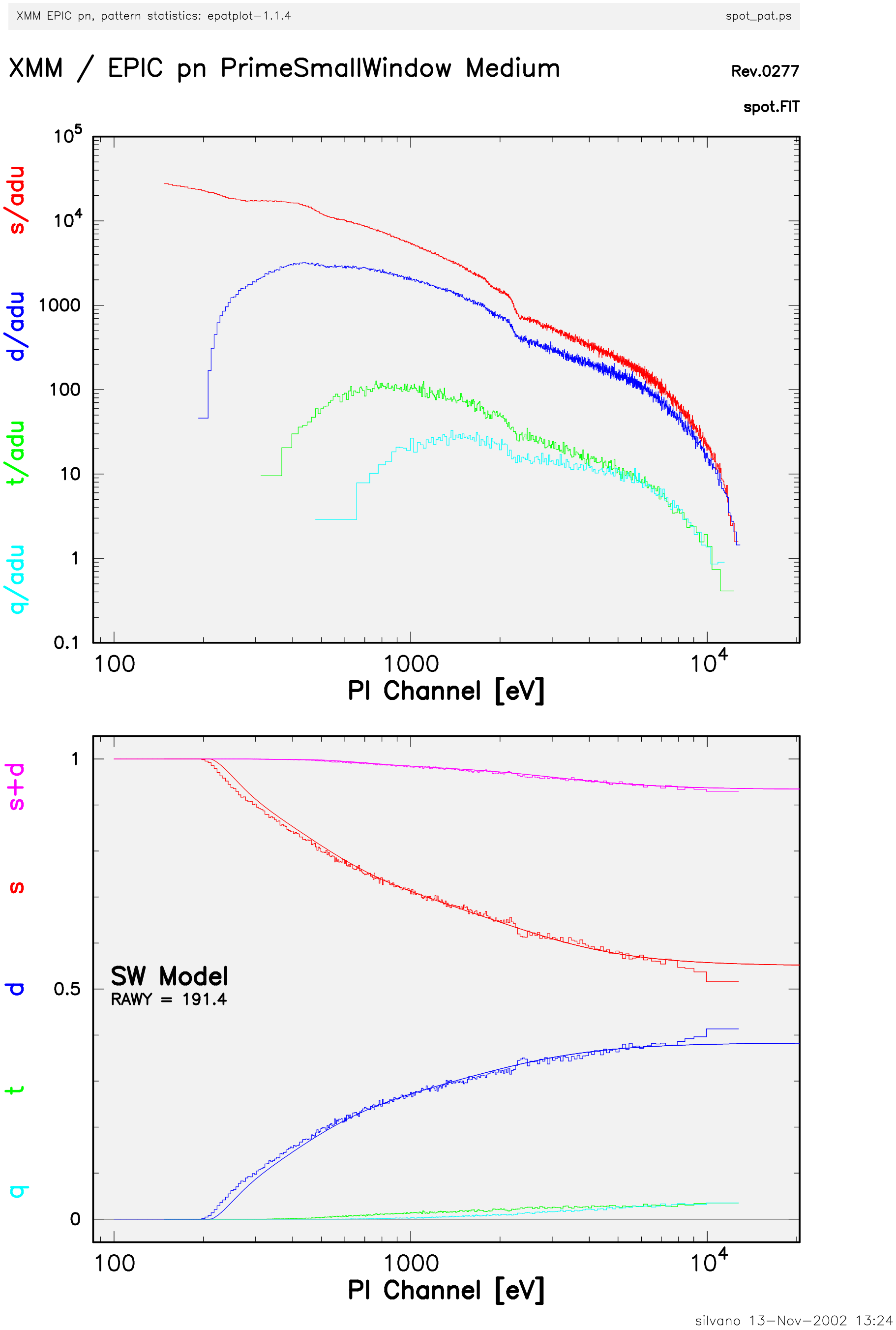

Figure 6: epatplot for a circle with radius 40″

reported in Table 4.

Table 4: Fits to PN spectra.

Spectrum	Γ 3-10 keV	Γ 4-10 keV
PN S 0″-40″	1.65 ± 0.01	1.67 ± 0.01
PN D 0″-40″	1.62 ± 0.01	1.62 ± 0.01
PN S 5″-40″	1.67 ± 0.01	1.72 ± 0.02
PN D 5″-40″	1.63 ± 0.01	1.66 ± 0.02
PN S 10″-40″	1.67 ± 0.01	1.72 ± 0.02
PN D 10″-40″	1.63 ± 0.01	1.66 ± 0.02

As can be seen there is a difference in the spectral slope recovered from singles and doubles. The difference is larger in the 4-10 keV fits than in the 3-10 keV fits. Inspection of the residuals shows that it is related to an excess in the doubles spectrum in the 8-10 keV band. Pile-up is unlikely to be a cause for this as the excess is observed in all the doubles spectra reported in Table 5. Interestingly, F. Haberl has recently reported that a similar effect has been observed in other sources, a likely origin could be a small error in the doubles to singles relative quantum efficency in the 8-10 keV range.

3 MECS

A BeppoSAX observation was carried out simultaneously with the XMM-Newton observation. The MECS instrument on-board BeppoSAX operating in the 2-10 keV band is well suited for a comparison with the EPIC MOS and PN hard bands. The MECS is a GSPC which has been extensively calibrated both on ground and in-flight.

We have performed spectral fits to the combined MECS2 and MECS3 spectrum produced by the standard pipeline at the BeppoSAX SDC in Rome. The extraction radius is 4′. The energy band used are as for EPIC 3-10 keV and 4-10 keV.

4 Comparing EPIC MOS, EPIC PN and MECS

In Table 5 we compare the results of EPIC PN, EPIC MOS and MECS spectral fits in the 3-10 keV and 4-10 keV. For MOS we report the pattern 0 spectra corrected for pile-up according to the procedure reported in Section 1; for PN we report PN singles and doubles spectra for the circle with a $40''$ extraction radius and for MECS the fits to the combined MECS2 and MECS3 spectrum produced by the standard pipeline at the BeppoSAX SDC in Rome.

Table 5: comparison between fits obtained with different instruments

Spectrum	Γ 3-10 keV	Γ 4-10 keV
MOS1 pat0 diacor	1.57 ± 0.02	1.67 ± 0.04
MOS2 pat0 diacor	1.65 ± 0.03	1.70 ± 0.04
PN S $0''$-$40''$	1.65 ± 0.01	1.67 ± 0.01
PN D $0''$-$40''$	1.62 ± 0.01	1.62 ± 0.01
MECS23	1.63 ± 0.02	1.64 ± 0.03

Let us first address the issue of the MOS PN cross-calibration. In the 3-10 keV band all measurements, except the MOS1, cluster within a $\Delta\Gamma$ of 0.03 and are consistent with one another at the 2.2σ level. The MOS1 slope is significantly harder than all others, $\Delta\Gamma \sim 0.07$. Interestingly when we go to the 4-10 keV band all measurements, including the MOS1, are contained within a $\Delta\Gamma$ of 0.08. Each measurement is consistent with any other at the 1σ level, with the exception of the PN singles and PN doubles measurements which differ at the 3.5 σ level (for more details on this see the PN section).

As far as the comparison with the BeppoSAX MECS is concerned, we find that in the 3-10 keV band all EPIC measurements, except for the MOS1, are in good agreement with the MECS measurement. For the 4-10 keV the MECS slope is consistent with all EPIC slopes, indeed the MECS 1σ confidence region encompasses all the EPIC measurements. Considering that BeppoSAX and ASCA are no longer operational and that Chandra's effective area drops sharply above 6 keV, the observation at hand is likely one of the best we have to perform a hard band cross-calibration between XMM-Newton EPIC and another X-ray experiment on a different observatory. Thus the fact that the

MECS measurements in the 3-10 keV and 4-10 keV band are consistent with all EPIC measurements, except of course the MOS1 measurement in the 3-10 keV band, implies that cross-calibration has been achieved to the available statistical level and that it is unlikely that BeppoSAX, or any other satellite for that matter, will be able to place more stringent constraints on spectral parameters derived with EPIC in the hard band. From now on efforts will have to be concentrated on improving the MOS / PN cross calibration. Here we are left with two problems: the MOS1 response in the 3-10 keV band and the PN singles and doubles inconsistency in the 4-10 keV band. Given these problems we may quantify the residual systematic indetermination on the spectral slope σ_Γ to be 0.02 in the 3-10 keV band (if we exclude the MOS1 result) and 0.04 in the 4-10 keV.

5 Summary

The main results of this Report may be summarized in the following bullets.

- MOS Spectra
  - At the observed rate of $\sim$ 17 cts/s MOS1 and MOS2 spectra show significant pile-up in the PSF core. This is borne out by the standard epatplot analysis, the pattern ratio analysis described in section 1.1, the pattern 0 vs. pattern 0-12 spectral fitting (section 1.2) and the diagonal pattern analysis (section 1.3).
  - In section 1.3 (see Appendices A and B for details) we provide a formula to correct pattern 0 spectra from pile-up. The formula can be used for any source provided that pile-up is relatively modest, (i.e. pile-ups involving 3 or more photons are neglected). Application of this formula to the MOS data shows that in the case at hand pattern 0 spectra are only mildly distorted by pile-up.
  - Pattern 0-12 spectra are substantially distorted by pile-up, measured spectral indices are flatter than they would be in the absence of pile-up and features appear at the position of the Si and Au and edges, these are due to piled up events which fill-up the sharp drops expected at these energies.
- PN Spectra

  – PN spectra are not significantly piled-up, this is borne out by the comparison of singles and doubles spectral fits and by the epatplot analysis.
  – PN doubles spectra are flatter ($\Delta\Gamma \sim 0.04$) than PN singles spectra, the most likely cause for this difference is a an error in the doubles to singles relative quantum efficency in the 8-10 keV range.

- MOS / PN cross calibration: in the 3-10 keV band MOS2, PN singles and PN doubles measurements are all found within a $\Delta\Gamma \sim 0.03$, only MOS1 returns a significantly flatter spectral slope.

- EPIC / MECS cross calibration: EPIC measurements, with the exception of the MOS1 measurement in the 3-10 keV band, are in good agreement with the MECS measurements.

Acknowledgments

It is a pleasure to acknowledge the many colleagues that have helped us. Thanks are due to to F. Haberl and M. Freyberg for the production of datasets and response matrices. M. Freyberg and B. Altrieri are thanked for their comments to a preliminary version of this report, and M. Turner for stimulating discussions on pile-up. Finally we are in debt with J.Ballet for a scrupulous reading of the manuscript, appendices included, which uncovered errors in some of the formulae.

A Appendix A

Let us consider the case of a source illuminating the MOS CCDs homogeneously. Let us also assume that the only form of pile-ups are two photon pile-ups (i.e. we neglect pile-ups due to 3 or more events). The spectrum of singles in the no pile-up limit $S(E)$ per frame per pixel may be written as:

$$S(E) = S_{obs}(E) + S_{lost}(E) - S_{gain}(E), \quad (A1)$$

where $S_{obs}(E)$ is the observed pattern 0 spectrum, $S_{lost}(E)$ is the spectrum "lost" to singles and higher order pattern pile-ups and $S_{gain}(E)$ is the spectrum gained from single-single pile-ups. The spectrum of events gained from pile-up $S_{gain}(E)$ can be expressed as a convolution of the non-piled up spectrum with itself.

$$S_{gain}(E) = \frac{1}{2}\int_{E_1} S(E_1)\cdot S(E-E_1)\ dE_1. \qquad (A2)$$

To derive the lost spectrum we must first recall that the loss of events does not result in a distortion of the spectra shape. Indeed the probability of an event to be piled-up is independent of its energy. Thus the loss will simply result in a reduction of the normalization of the spectrum which can be readily estimated from the formulae reported in Ballet (1999). The rate of recorded monopixels events per frame per pixel can be expressed as:

$$\mu_1 = (e^{\alpha_1\lambda}-1)e^{-\gamma_1\lambda} \qquad (A3),$$

where: λ is the in-coming X-ray flux/pixel/frame, $\gamma_1 = 9{+}3\alpha_2{+}6\alpha_3{+}7\alpha_4$ and α_1, α_2, α_3 and α_4 are the fraction of events giving rise to monopixels, bipixels tripixels and quadripixels in the no pile-up limit, Since the above parameters vary with energy, their actual values are computed by averaging over the whole spectral range. Equation (A3) is easily understood, if we expand the first term in a Taylor series we find $\alpha_1\lambda + (\alpha_1\lambda)^2/2+\,(\alpha_1\lambda)^3/3+$ ... the first term in the expansion is the expected rate in the no pile-up limit, the second term accounts for the gain from 2 photon pile-up, the third term for the gain from 3 photon pile-up and so on. The second term in Eq. (A3), $e^{-\gamma_1\lambda}$, is a loss term, in the no pile-up limit it reduces to 1. For modest pile-up it may be expressed as $(1-\gamma_1\lambda)$, where $\gamma_1\lambda$ accounts for the events which have been lost to form piled up singles doubles tripixels and quadripixels. Under this condition the rate of lost events may be written as $\mu_{1\_lost} = \gamma_1\alpha_1\lambda^2$. Similarly it can be shown that the spectrum of lost events may be expressed as:

$$S_{lost}(E) = \frac{\gamma_1}{\alpha_1}\ (\alpha_1\lambda)\ S(E), \qquad (A4)$$

where $\alpha_1\lambda = \int_E S(E)dE$ and $\int_E S_{lost}(E)dE = \mu_{1\_lost}$.

Both the spectrum of gained events, $S_{gain}(E)$, and lost events, $S_{lost}(E)$, can be estimated from the spectrum of diagonal events (patterns 26-29). To avoid confusion we shall call $S_{dia}(E)$ the spectrum observed in diagonal patterns and $S_{dia\_p0}(E)$ the spectrum of pattern 0 reconstructed by splitting each diagonal event into two pattern 0 events. As far as the $S_{gain}(E)$ term is concerned we recall that diagonals are produced from the pile-up of two pattern 0 events just as piled-up singles. Thus the difference is only in the normalization, which for diagonals is 4 times larger to account for the 4 possible positions of the second event giving rise to the diagonal. We may then write:

$$S_{gain}(E) = \frac{1}{4} S_{dia}(E). \qquad (A5)$$

Similarly $S_{lost}(E)$ may be related to $S_{dia\_p0}(E)$, if we recall that lost single events are either lost to permitted singles, doubles, tripixels and quadripixels or to diagonals, i.e.: $S_{lost}(E) = S_{per\_p0}(E) + S_{dia\_p0}(E)$, where $S_{per\_p0}(E)$ is the spectrum lost to permitted patterns and $S_{dia\_p0}(E)$ is the spectrum lost to diagonals. $S_{per\_p0}(E)$ and $S_{dia\_p0}(E)$ are related to $S(E)$ as follows:

$$S_{per\_p0}(E) = \gamma_{1\_p} \lambda S(E), \qquad S_{dia\_p0}(E) = \gamma_{1\_d} \lambda S(E),$$

where the loss coefficient γ_{1_d}, which may be derived from Eq. (A3) or (A4) of Ballet (1999) is $\gamma_{1\_d} = 4\alpha_1$ and γ_{1_p} is obtained from the relation $\gamma_{1\_p} = \gamma_1 - \gamma_{1\_d}$. From the above it follows that $S_{lost}(E)$ may be easily re-written in terms of $S_{dia\_p0}(E)$:

$$S_{lost}(E) = \frac{\gamma_1}{4\alpha_1} S_{dia\_p0}(E). \qquad (A6)$$

B Appendix B

The equations derived in Appendix A refer to the case of a source illuminating the MOS CCDs homogeneously. In this Appendix we shall see how they may be extended to a generic point source with a surface brightness described by the MOS PSF. Let us start by defining $S(E, r)$ as the spectrum per pixel per frame at the radial distance r from the center of the surface brightness distribution in the no pile-up limit.

Since the size of the MOS pixels is smaller than the PSF of the XMM telescope the equations derived in Appendix A are all applicable locally. For instance we may write:

$$S(E, r) = S_{obs}(E, r) + S_{lost}(E, r) - S_{gain}(E, r). \qquad (B1)$$

In the case of $S_{gain}(E,r)$ we may write:

$$S_{gain}(E,r) = \frac{1}{2}\int_{E_1} S(E_1,r)\cdot S(E-E_1,r)\ dE_1. \qquad (B2)$$

We may define a mean spectrum as follows:

$$\bar{S}_{gain}(E) \equiv \frac{\int_{r_{min}}^{r_{max}} 2\pi r dr S_{gain}(E,r)}{\int_{r_{min}}^{r_{max}} 2\pi r dr}. \qquad (B3)$$

As for other equations derived in Appendix A Eq. (A5) applies locally. i.e.:

$$S_{gain}(E,r) = \frac{1}{4} S_{dia}(E,r). \qquad (B4)$$

Substituting Eq. (B4) in (B3) and defining

$$\bar{S}_{dia}(E) \equiv \frac{\int_{r_{min}}^{r_{max}} 2\pi r dr S_{dia}(E,r)}{\int_{r_{min}}^{r_{max}} 2\pi r dr}, \qquad (B5)$$

we obtain the generalization of Eq. (A5):

$$\bar{S}_{gain}(E) = \frac{1}{4}\bar{S}_{dia}(E). \qquad (B6)$$

Similarly if we define

$$\bar{S}_{lost}(E) \equiv \frac{\int_{r_{min}}^{r_{max}} 2\pi r dr S_{lost}(E,r)}{\int_{r_{min}}^{r_{max}} 2\pi r dr}, \qquad (B7)$$

assume Eq. (A6) to be valid locally, i.e.

$$S_{lost}(E,r) = \frac{\gamma_1}{4\alpha_1} S_{dia\_p0}(E,r), \qquad (B8)$$

and define

$$\bar{S}_{dia\_p0}(E) \equiv \frac{\int_{r_{min}}^{r_{max}} 2\pi r dr S_{dia\_p0}(E,r)}{\int_{r_{min}}^{r_{max}} 2\pi r dr}, \qquad (B9)$$

we derive the generalization of Eq. (A6):

$$\bar{S}_{lost}(E) = \frac{\gamma_1}{4\alpha_1}\bar{S}_{dia\_p0}(E). \qquad (B10)$$

Integrating Eq. (B1) over the source surface brightness we derive

$$\bar{S}(E) = \bar{S}_{obs}(E) + \bar{S}_{lost}(E) - \bar{S}_{gain}(E), \qquad (B11)$$

finally substituting Eq. (B6) and (B8) in (B11) we obtain

$$\bar{S}(E) = \bar{S}_{obs}(E) + \frac{\gamma_1}{4\alpha_1}\bar{S}_{dia\_p0}(E) - \frac{1}{4}\bar{S}_{dia}(E). \qquad (B12)$$